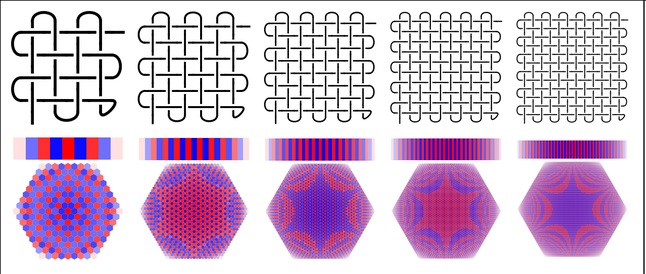

FIGURE 1.2. Θ of some square weave knots, as computed by [BV3, WeaveKnots.nb].

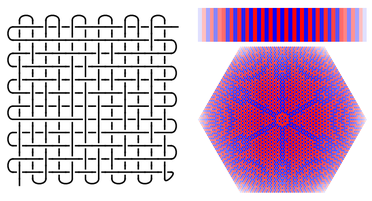

FIGURE 1.3. Θ of a randomized weave knot, as computed by [BV3, WeaveKnots.nb]. Crossings were chosen to be positive or negative with equal probabilities.

2. The Main Theorem

We start with the definition of Θ. Given an oriented n-crossing knot K, we draw it in the plane as a long knot diagram D in such a way that the two strands intersecting at each crossing are pointing up (that's always possible because we can always rotate crossings as needed), and so that at its beginning and at its end the knot is oriented upward. We call such a diagram an *upright knot diagram*. An example of an upright knot diagram is shown on the right.

We then label each edge of the diagram with two labels: a running index k which runs from 1 to $2n+1$, and a "rotation number" φ_k, the geometric rotation number of that edge[1]. In

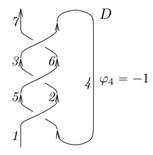

FIGURE 2.1. An example upright knot diagram.

[1]The signed number of times the tangent to the edge is horizontal and heading right, with cups counted with +1 signs and caps with −1; this number is well defined because at their ends, all edges are headed up.

In particular, the middle diagram which resembles the Greek letter Θ gave the invariant its name. [4]

Comment 5. The computation of G is a bottleneck for the computation of Θ. It requires inverting a $(2n+1)\times(2n+1)$ matrix whose entries are (degree 1) Laurent polynomials in T. It's a daunting task yet it takes polynomial time. Even a naive inversion using Gaussian elimination requires only $\sim n^3$ operations in the ring $\mathbb{Q}(T)$. So G can be computed in practice even if n is in the hundreds, and everything which then follows is not worse.

The polynomials $F_1(c)$, $F_2(c_0,c_1)$ and $F_3(k)$ are not unique, and we are not certain that we have the cleanest possible formulas for them. They are ugly from a human perspective, yet from a computational perspective, having 18 terms (as is the case for $F_1(c)$) isn't really a problem; computers don't care.

Computationally, the worst term in (6) is the middle one, and even it takes merely $\sim n^2$ operations in the ring $\mathbb{Q}(T_1,T_2)$ to evaluate. [5]

3. Implementation and Examples

3.1. **Implementation.** A concise yet reasonably efficient implementation is worth a thousand formulas. It completely removes ambiguities, it tests the theories, and it allows for experimentation. Hence our next task is to implement. The section that follows was generated from a Mathematica [Wo] notebook which is available at [BV3, Theta.nb]. A second implementation of Θ, using Python and SageMath (https://www.sagemath.org/) is available at https://www.rolandvdv.nl/Theta/.

We start by loading the package `KnotTheory‘` — it is only needed because it has many specific knots pre-defined. In this Section and in the next, ☺ and ☺ mean "human input" while 💻 means "computer output":

```
In  Once[<< KnotTheory`]
Out Loading KnotTheory` version of October 29, 2024, 10:29:52.1301.
    Read more at http://katlas.org/wiki/KnotTheory.
```

Next we quietly define the modules `Rot`, used to compute rotation numbers, and `PolyPlot`, used to plot polynomials as bar codes and as hexagonal QR codes. Neither is a part of the core of the computation of Θ, so neither is shown; yet we do show one usage example for each.

```
In  (* The definitions of Rot and PolyPlot are suppressed *)
In  Rot[Mirror@Knot[3, 1]]
Out {{{1, 1, 4}, {1, 3, 6}, {1, 5, 2}}, {0, 0, 0, -1, 0, 0, 0}}
```

We urge the reader to compare the above output with the knot diagram in Figure 2.1.

```
In  PolyPlot[{2 T - 1 + T^-1, -1 + T1 - 2 T2 + 4 T1^-1 T2^-1},
      ImageSize → 100, Labeled → True]
```

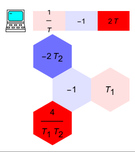


```
In  ImageCompose[PolyPlot[Θ[TorusKnot[22, 7]], ImageSize → 720],
      TubePlot[TorusKnot[22, 7], ImageSize → 360], {Right, Bottom}, {Right, Bottom}]
```

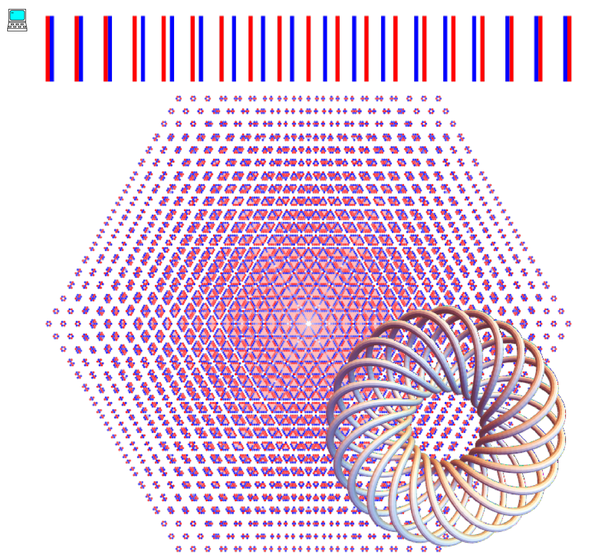

FIGURE 3.1. The 132-crossing torus knot $T_{22/7}$ and a plot of its Θ invariant

i^+ (these are $i+1$ and $i+2$ if the labelling is by consecutive integers). Also, by convention "1" will always refer to the label of the first edge, and "$2n+1$" will always refer to the label of the last. With this in mind, we have that $A = I + \sum_c A_c$, with A_c given by

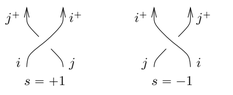

$\longrightarrow$

A_c	column i^+	column j^+
row i	$-T^s$	T^s-1
row j	0	−1

(7)

Like in [BV1, Lemma 3], the equalities $AG=I$ and $GA=I$ imply that for any crossing $c=(s,i,j)$ in a knot diagram D, the Green function $G=(g_{\alpha\beta})$ of D satisfies the following

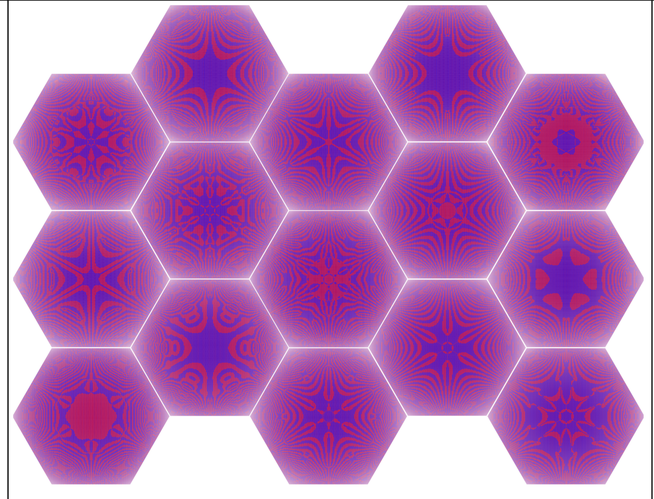

FIGURE 1.4. θ (hexagonal QR code only) of the 15 largest knots that we have computed by September 16, 2024. They are all "generic" in as much as we know, and they all have ⩾ 300 crossings. The knots come from [DHOEBL]. Warning: Some screens/printers may introduce spurious Moiré interference patterns.

Figure 2.1 the running index runs from 1 to 7, and the rotation numbers for all edges are 0 (and hence are omitted) except for φ_4, which is −1.

Let X be the set of all crossings in the diagram D, where we encode each crossing as a triple (sign of the crossing, incoming over edge, incoming under edge). In our example we have $X=\{(1,1,4),(1,5,2),(1,3,6)\}$.

We let A be the $(2n+1)\times(2n+1)$ matrix of Laurent polynomials in a variable T, defined by

$$A := I - \sum_{c=(s,i,j)\in X} \left(T^s E_{i,i+1} + (1-T^s)E_{i,j+1} + E_{j,j+1}\right),$$

where I is the identity matrix and $E_{\alpha\beta}$ denotes the elementary matrix with 1 in row α and column β and zeros elsewhere.

Alternatively, $A = I + \sum_c A_c$, where A_c is a matrix of zeros except for the blocks as follows:

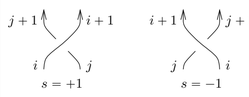

$\longrightarrow$

A_c	column $i+1$	column $j+1$
row i	$-T^s$	T^s-1
row j	0	−1

(1)

We note that the determinant of A is equal up to a unit to the normalized Alexander polynomial Δ of K.[2] In fact, we have that

$$\Delta = \Delta(K) = T^{(-\varphi(D)-w(D))/2}\det(A), \tag{2}$$

where $\varphi(D) := \sum_k \varphi_k$ is the total rotation number of D and where $w(D) = \sum_c s_c$ is the writhe of D, namely the sum of the signs s_c of all the crossings c in D.

We let $G = (g_{\alpha\beta}) = A^{-1}$, and, thinking of it as a function $g_{\alpha\beta}$ of a pair of edges α and β, we call it the Green function of the diagram D. When inspired by physics (e.g. Fact 33 and [BN6]) we sometimes call it "the 2-point function", and when thinking of car traffic (e.g. Comment 3 and [BV1, BN7]) we sometimes call it "the traffic function". As an example, here are A and G for the knot diagram D of Figure 2.1:

$$\begin{pmatrix} 1 & -T & 0 & 0 & T-1 & 0 & 0 \\ 0 & 1 & -1 & 0 & 0 & 0 & 0 \\ 0 & 0 & 1 & -T & 0 & 0 & T-1 \\ 0 & 0 & 0 & 1 & -1 & 0 & 0 \\ 0 & 0 & T-1 & 0 & 1 & -T & 0 \\ 0 & 0 & 0 & 0 & 0 & 1 & -1 \\ 0 & 0 & 0 & 0 & 0 & 0 & 1 \end{pmatrix}, \quad \begin{pmatrix} 1 & T & 1 & T & 1 & T & 1 \\ 0 & 1 & \frac{1}{T^2-T+1} & \frac{T}{T^2-T+1} & \frac{T}{T^2-T+1} & \frac{T^2}{T^2-T+1} & 1 \\ 0 & 0 & \frac{1}{T^2-T+1} & \frac{T}{T^2-T+1} & \frac{T}{T^2-T+1} & \frac{T^2}{T^2-T+1} & 1 \\ 0 & 0 & \frac{1-T}{T^2-T+1} & \frac{1-T}{T^2-T+1} & \frac{1-T}{T^2-T+1} & \frac{T}{T^2-T+1} & 1 \\ 0 & 0 & \frac{1-T}{T^2-T+1} & \frac{T-T^2}{T^2-T+1} & \frac{1}{T^2-T+1} & \frac{T}{T^2-T+1} & 1 \\ 0 & 0 & 0 & 0 & 0 & 1 & 1 \\ 0 & 0 & 0 & 0 & 0 & 0 & 1 \end{pmatrix}.$$

Let T_1 and T_2 be indeterminates and let $T_3 := T_1T_2$. Let $\Delta_\nu := \Delta|_{T\to T_\nu}$ and $G_\nu = (g_{\nu\alpha\beta}) := G|_{T\to T_\nu}$ be Δ and G subject to the substitution $T\to T_\nu$, where $\nu = 1,2,3$.

Given crossings $c=(s,i,j)$, $c_0=(s_0,i_0,j_0)$, and $c_1=(s_1,i_1,j_1)$ in X and an edge label k, let

$$\begin{aligned} F_1(c) = s\,[&1/2 - g_{3ii} + T_2^s g_{1ii}g_{2ji} - T_2^s g_{3jj}g_{2ji} - (T_2^s-1)g_{3ii}g_{2ji} \\ &+(T_3^s-1)g_{2ji}g_{3ji} - g_{1ii}g_{2jj} + 2g_{3ii}g_{2jj} + g_{1ii}g_{3jj} - g_{2ii}g_{3jj}] \\ &+ \frac{s}{T_2^s-1}\,[(T_1^s-1)T_2^s\,(g_{3jj}g_{1ji} - g_{2jj}g_{1ji} + T_2^s g_{1ji}g_{2ji}) \\ &+ (T_3^s-1)g_{3ji}\,(1 - T_2^s g_{1ii} + g_{2ij} + (T_2^s-2)g_{2jj} - (T_1^s-1)(T_2^s+1)g_{1ji})] \end{aligned} \tag{3}$$

$$F_2(c_0,c_1) = \frac{s_1(T_1^{s_0}-1)(T_3^{s_1}-1)g_{1j_1i_0}g_{3j_0i_1}}{T_2^{s_1}-1}\,(T_2^{s_0}g_{2i_1i_0} + g_{2j_1j_0} - T_2^{s_0}g_{2j_1i_0} - g_{2i_1j_0}) \tag{4}$$

$$F_3(k) = (g_{3kk} - 1/2)\varphi_k \tag{5}$$

These formulas are uninspiring, yet they are easy to compute (given G), and they work:

[2]The informed reader will note that A is a presentation matrix for the Alexander module of K, obtained by using Fox calculus on the Wirtinger presentation of the fundamental group of the complement of K.

The definition of `CF` below is a technicality telling the computer how to best store polynomials in the $g_{\nu\alpha\beta}$'s such as F_1 and F_2. The programs would run just the same without it, albeit a bit more slowly:

```
In  CF[ℰ_] := Expand@Collect[ℰ, g__, F] /. F → Factor;
```

Next, we decree that $T_3 = T_1T_2$ and define the three "Feynman Diagram" polynomials F_1, F_2, and F_3:

```
In  T3 = T1 T2;
In  F1[{s_, i_, j_}] := CF[
      s (1/2 - g3ii + T2^s g1ii g2ji - g1ii g2jj - (T2^s - 1) g2ji g3ii + 2 g2jj g3ii - (1 - T3^s) g2ji g3ji -
         g2ii g3jj - T2^s g2ji g3jj + g1ii g3jj +
         ((T1^s - 1) g1ji (T2^2^s g2ji - T2^s g2jj + T2^s g3jj) +
            (T3^s - 1) g3ji (1 - T2^s g1ii + g2ij + (T2^s - 2) g2jj - (T1^s - 1) (T2^s + 1) g1ji)) / (T2^s - 1))]
In  F2[{s0_, i0_, j0_}, {s1_, i1_, j1_}] :=
      CF[s1 (T1^s0 - 1) (T2^s1 - 1)^-1 (T3^s1 - 1) g1,j1,i0 g3,j0,i1
         ((T2^s0 g2,i1,i0 - g2,i1,j0) - (T2^s0 g2,j1,i0 - g2,j1,j0))]
In  F3[{φ_, k_}] = φ g3kk - φ / 2;
```

Next comes the main program computing $\Theta(K)$. Fortunately, it matches perfectly with the mathematical description in Section 2. In line 1 below we use `Rot` to let X and φ be the crossings and rotation numbers of K. In addition we let n be the length of X, namely, the number of crossings in K, and we let the starting value of A be the $(2n+1)\times(2n+1)$ identity matrix. Then in line 2, for each crossing in X we add to A a 2×2 block, in rows i and j and columns $i+1$ and $j+1$, as explain in Equation (1). In line 3 we compute the normalized Alexander polynomial Δ as in (2). In line 4 we let G be the inverse of A. In line 5 we declare what it means to evaluate, `ev`, a formula $\mathcal{E}$ that may contain symbols of the form $g_{\nu\alpha\beta}$: each such symbol is to be replaced by the entry in position α,β of G, but with T replaced with T_ν. In line 6 we start computing θ by computing the first summand in (6), which in itself, is a sum over the crossings of the knot. In line 7 we add to θ the double sum corresponding to the second term in (6), and in line 8, we add the third summand of (6). Finally, line 9 outputs a pair: Δ, and the re-normalized version of θ.

```
In  Θ[K_] := Θ[K] = Module[{X, φ, n, A, Δ, G, ev, θ, k, k1, k2},
      (* 1 *) {X, φ} = Rot[K]; n = Length[X]; A = IdentityMatrix[2 n + 1];
      (* 2 *) Cases[X, {s_, i_, j_}] :→ (A[[{i, j}, {i + 1, j + 1}]] += (-T^s  T^s - 1
                                                                          0      -1 ));
      (* 3 *) Δ = T^(-Total[φ]-Total[X[All,1]])/2 Det[A];
      (* 4 *) G = Inverse[A];
      (* 5 *) ev[ℰ_] := Factor[ℰ /. g_ν_,α_,β_ :→ (G[[α, β]] /. T → T_ν)];
      (* 6 *) θ = ev[Sum[F1[X[[k]], {k, n}]]];
      (* 7 *) θ += ev[Sum[F2[X[[k1]], X[[k2]]], {k1, n}, {k2, n}]];
      (* 8 *) θ += ev[Sum[F3[φ[[k]], k], {k, Length@φ}]];
      (* 9 *) Factor@{Δ, (Δ /. T → T1) (Δ /. T → T2) (Δ /. T → T3) θ}
      ];
```

3.2. **Examples.** On to examples! Starting with the trefoil knot.

```
In  Expand[Θ[Knot[3, 1]]]
```

$$\left\{-1 + \frac{1}{T} + T,\ -\frac{1}{T_1^2} - T_1^2 - \frac{1}{T_2^2} - \frac{1}{T_1^2T_2^2} + \frac{1}{T_1T_2^2} + \frac{1}{T_1^2T_2} + \frac{T_1}{T_2} + \frac{T_2}{T_1} + T_1^2T_2 - T_2^2 + T_1T_2^2 - T_1^2T_2^2\right\}$$

```
In  PolyPlot[Θ[Knot[3, 1]], ImageSize → Tiny]
```

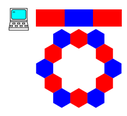

Next are the Conway knot 11_{n34} and the Kinoshita-Terasaka knot 11_{n42}. The two are mutants and famously hard to separate: they both have $\Delta = 1$ (as evidenced by their one-bar Alexander bar codes below), and they have the same hyperbolic volume, HOMFLY-PT polynomial, and Khovanov homology. Yet their θ invariants are different. Note that the genus of the Conway knot is 3, while the genus of the Kinoshita-Terasaka knot is 2. This agrees with the apparent higher complexity of the QR code of the Conway polynomial and with Conjecture 18 below.

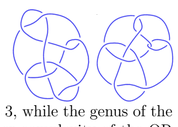

```
In  PolyPlot[Θ[Knot[#]], ImageSize → 120] & /@
      {"K11n34", "K11n42"}
```

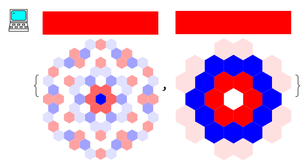

Torus knots have particularly nice-looking Θ invariants. Here are the torus knots $T_{13/2}$, $T_{17/3}$, $T_{13/5}$, and $T_{7/6}$:

```
In  ImageCompose[PolyPlot[Θ[TorusKnot @@ #], ImageSize → 480],
      TubePlot[TorusKnot @@ #, ImageSize → 240], {Right, Bottom}, {Right, Bottom}] & /@
      {{13, 2}, {17, 3}, {13, 5}, {7, 6}} // GraphicsRow
```

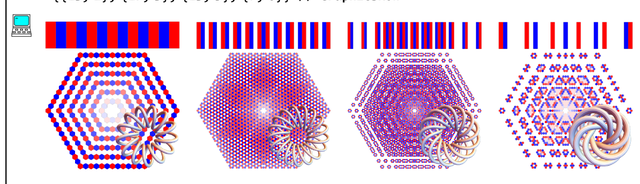

The next line shows the computation time in seconds for the 132-crossing torus knot $T_{22/7}$ on a 2024 laptop, without actually showing the output. The output plot is in Figure 3.1.

```
In  AbsoluteTiming[Θ[TorusKnot[22, 7]];]
Out {1020.73, Null}
```

We note that if T_1 and T_2 are assigned specific rational numbers and if the program for Θ is slightly modified so as to compute each G_ν separately (rather than computing G symbolically and then substituting $T\to T_\nu$), then the program becomes significantly more efficient, for inverting a numerical matrix is cheaper than inverting a symbolic matrix (but then one obtains numerical answers and the beauty and the topological significance (Section 5) are lost). The Mathematica notebook that accompanies this paper, [BV3, Theta.nb], contains the required modified program as well as a few computational examples. One finds that with $T_1 = 22/7$ and $T_2 = 21/13$, the invariant Θ can be computed for knots with 600 crossings, and that for knots with up to 15 crossings, its separation power remains the same.

If T_1 and T_2 are assigned approximate real values, say π and e computed to 100 decimal digits, then Θ can be computed on knots with 1,000 crossings and, for knots with up to 15 crossings it remains very strong. But approximate real numbers are a bit thorny. It is hard to know how far one needs to compute before deciding that two such numbers are equal, and when two such numbers appear unequal, it is hard to tell if that is merely because they were computed differently and different roundings were applied. Thorns and snares are in the way of the perverse; He who guards his soul will be far from them (Proverbs 22:5)[3].

4. Proof of the Main Theorem, Theorem 1

We divide the proof into to parts: the invariance of θ_0 (and therefore of θ) is in Section 4.1, and the polynomiality of θ is in Section 4.2.

4.1. **Proof of Invariance.** Our proof of the invariance of θ (Theorem 1) is very similar, and uses many of the same pieces, as the proof of the invariance of ρ_1 in [BV1]. Thus at some places here we are briefer than at [BV1], and sadly, yet in the interest of saving space, we understate here the interpretation of $g_{\alpha\beta}$ as a "traffic function".

Some Reidemeister moves create or lose an edge and to avoid the need for renumbering it is beneficial to also allow labelling the edges with non-consecutive labels. Hence we allow that, and write i^+ for the successor of the label i along the knot, and i^{++} for the successor of

[3] שומר נפשו ירחק.

Theorem 1 (The Main Theorem, proof in Section 4)**.** *The following are knot invariants:*

$$\theta_0(D) := \sum_{c\in X} F_1(c) + \sum_{c_0,c_1\in X} F_2(c_0,c_1) + \sum_{\text{edges } k} F_3(k) \quad \text{and} \quad \theta(D) := \Delta_1\Delta_2\Delta_3\theta_0(D). \tag{6}$$

Furthermore, θ is a Laurent polynomial in T_1 and T_2, with integer coefficients.

Some comments are now in order:

Comment 2. The entries of G_ν are rational functions with denominators Δ_ν, and so θ_0 is valued in the ring of rational functions $\mathbb{Q}(T_1,T_2)$. The point of θ is to clear these denominators by multiplying by $\Delta_1\Delta_2\Delta_3$ so as to get an invariant valued in Laurent polynomials. (There remains a potential denominator of the form $(T_2-1)^{-1}$ coming from the explicit denominators in Equations (3) and (4). It will be shown to cancel in Section 4.2.)

Comment 3. We note following [BV1] that $g_{\alpha\beta}$ can be interpreted as measuring "car traffic", assuming a stream of traffic is injected near the start of edge α and a "traffic counter" is placed near the end of edge β, and where cars always obey the following traffic rules:

- Car travel on the edges of the knot, always in a direction consistent with the orientation of these edges.
- When a car reaches a crossing on the under-strand, it travels through and continues on the other side.
- When a car reaches a crossing of sign $s=\pm1$ on the over-strand, it continues right through with probability T^s, yet with probability $1-T^s$ it falls down and continues travelling on the lower strand. (It matters not that T and T^{-1} cannot be between 0 and 1 at the same time — we merely use the algebraic rules of probability without caring about the inequalities that normally come with them).
- When cars reach the "end" of the knot, the abyss that follows edge $2n+1$, they fall off the picture never to be seen again.

These rules can be summarized by the following pictures:

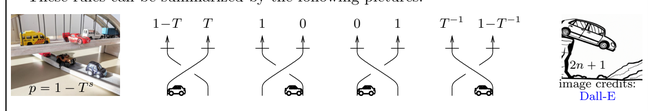

For further details, see [BV1]. [3]

Comment 4. We note without detail that there is an alternative formula for θ in terms of perturbed Gaussian integration [BN6]. In that language, and using also the traffic motifs of Discussion 3, the three summands in (6) become Feynman diagrams for processes in which cars 🚗$_\nu$ governed by parameter $T_\nu = T_1, T_2$, or T_3 interact:

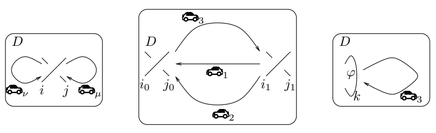

The next line shows the computation time in seconds for the 132-crossing torus knot $T_{22/7}$ on a 2024 laptop, without actually showing the output. The output plot is in Figure 3.1.

```
In  AbsoluteTiming[Θ[TorusKnot[22, 7]];]
Out {1020.73, Null}
```

We note that if T_1 and T_2 are assigned specific rational numbers and if the program for Θ is slightly modified so as to compute each G_ν separately (rather than computing G symbolically and then substituting $T\to T_\nu$), then the program becomes significantly more efficient, for inverting a numerical matrix is cheaper than inverting a symbolic matrix (but then one obtains numerical answers and the beauty and the topological significance (Section 5) are lost). The Mathematica notebook that accompanies this paper, [BV3, Theta.nb], contains the required modified program as well as a few computational examples. One finds that with $T_1 = 22/7$ and $T_2 = 21/13$, the invariant Θ can be computed for knots with 600 crossings, and that for knots with up to 15 crossings, its separation power remains the same.

If T_1 and T_2 are assigned approximate real values, say π and e computed to 100 decimal digits, then Θ can be computed on knots with 1,000 crossings and, for knots with up to 15 crossings it remains very strong. But approximate real numbers are a bit thorny. It is hard to know how far one needs to compute before deciding that two such numbers are equal, and when two such numbers appear unequal, it is hard to tell if that is merely because they were computed differently and different roundings were applied. Thorns and snares are in the way of the perverse; He who guards his soul will be far from them (Proverbs 22:5)[3].

4. Proof of the Main Theorem, Theorem 1

We divide the proof into to parts: the invariance of θ_0 (and therefore of θ) is in Section 4.1, and the polynomiality of θ is in Section 4.2.

4.1. **Proof of Invariance.** Our proof of the invariance of θ (Theorem 1) is very similar, and uses many of the same pieces, as the proof of the invariance of ρ_1 in [BV1]. Thus at some places here we are briefer than at [BV1], and sadly, yet in the interest of saving space, we understate here the interpretation of $g_{\alpha\beta}$ as a "traffic function".

Some Reidemeister moves create or lose an edge and to avoid the need for renumbering it is beneficial to also allow labelling the edges with non-consecutive labels. Hence we allow that, and write i^+ for the successor of the label i along the knot, and i^{++} for the successor of

i^+ (these are $i+1$ and $i+2$ if the labelling is by consecutive integers). Also, by convention "1" will always refer to the label of the first edge, and "$2n+1$" will always refer to the label of the last. With this in mind, we have that $A = I + \sum_c A_c$, with A_c given by

$\longrightarrow$

A_c	column i^+	column j^+
row i	$-T^s$	T^s-1
row j	0	−1

(7)

Like in [BV1, Lemma 3], the equalities $AG=I$ and $GA=I$ imply that for any crossing $c=(s,i,j)$ in a knot diagram D, the Green function $G=(g_{\alpha\beta})$ of D satisfies the following

$$\begin{aligned} g_{i,\beta} &= \delta_{i\beta} + T^2 g_{i^{++},\beta} + T(1-T)g_{j^{++},\beta} + (1-T)g_{k^{++},\beta}, \\ g_{j,\beta} &= \delta_{j\beta} + Tg_{j^{++},\beta} + (1-T)g_{k^{++},\beta}, \qquad g_{k,\beta} = \delta_{k\beta} + g_{k^{++},\beta}, \end{aligned} \tag{13}$$

$$g_{i^+,\beta} = Tg_{i^{++},\beta} + (1-T)g_{j^{++},\beta}, \qquad g_{j^+,\beta} = g_{j^{++},\beta}, \qquad g_{k^+,\beta} = g_{k^{++},\beta}. \tag{14}$$

In this system the indices i^+, j^+ and k^+ do not appear in (13) or in the further g-rules corresponding to the further crossings. Hence for the purpose of determining $g_{\alpha\beta}$ with $\alpha,\beta\notin\{i^+,j^+,k^+\}$, Equations (14) can be ignored.

Similarly eliminating $g'_{i^+,\beta}$, $g'_{j^+,\beta}$, and $g'_{k^+,\beta}$ from the second set of equations, we find that it is equivalent to

$$\begin{aligned} g'_{i,\beta} &= \delta_{i\beta} + T^2 g'_{i^{++},\beta} + T(1-T)g'_{j^{++},\beta} + (1-T)g'_{k^{++},\beta}, \\ g'_{j,\beta} &= \delta_{j\beta} + Tg'_{j^{++},\beta} + (1-T)g'_{k^{++},\beta}, \qquad g'_{k,\beta} = \delta_{k\beta} + g'_{k^{++},\beta}, \end{aligned} \tag{15}$$

$$g'_{i^+,\beta} = Tg'_{i^{++},\beta} + (1-T)g'_{k^{++},\beta}, \qquad g'_{j^+,\beta} = Tg'_{j^{++},\beta} + (1-T)g'_{k^{++},\beta}, \qquad g'_{k^+,\beta} = g'_{k^{++},\beta}. \tag{16}$$

Using the same logic as before, for the purpose of determining $g'_{\alpha\beta}$ with $\alpha,\beta\notin\{i^+,j^+,k^+\}$, Equations (16) can be ignored.

But now we compare the unignored equations, (13) and (15), and find that they are exactly the same, except with $g\leftrightarrow g'$, and the same is true for the further g-rules and/or g'-rules coming from the further crossings. Hence so long as $\alpha,\beta\notin\{i^+,j^+,k^+\}$, we have that $g_{\alpha\beta} = g'_{\alpha\beta}$. In the case of the R3b move no edges merge or break up, and hence this implies that $\tilde g_{ab} = \tilde g'_{ab}$ so long as a and b are away from the move.

Next we deal with the case of R2c$^+$. We use the privileges afforded to us by Lemma 7 to insert 4 null vertices into the right-hand-side of the move, and like in the case of R3b, we start with pictures annotated with the relevant type (8) and (11) g-rules, written with the assumption that $\beta\notin\{i^+,j^+\}$:

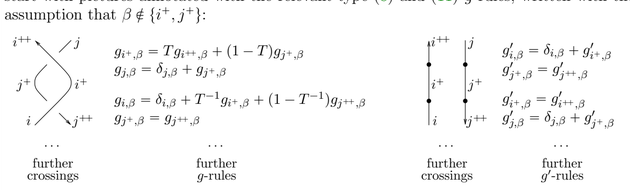

As in the case of R3b, we eliminate $g_{i^+,\beta}$ and $g_{j^+,\beta}$ from the equations for the left hand side, and find that for the purpose of determining $g_{\alpha\beta}$ with $\beta\notin\{i^+,j^+\}$, they are equivalent to the equations

$$g_{i,\beta} = \delta_{i,\beta} + g_{i^{++},\beta} \quad \text{and} \quad g_{j,\beta} = \delta_{j,\beta} + g_{j^{++},\beta}.$$

Likewise, the right hand side is clearly equivalent to

$$g'_{i,\beta} = \delta_{i,\beta} + g'_{i^{++},\beta} \quad \text{and} \quad g'_{j,\beta} = \delta_{j,\beta} + g'_{j^{++},\beta},$$

and as in the case of R3b, this establishes the invariance of $\tilde g_{ab}$ under R2c moves.

For the remaining moves, R2c$^-$, R1l, and R1r, we merely display the g-rules and leave it to the readers to verify that when the edges i^+ and/or j^+ are eliminated, the left hand sides

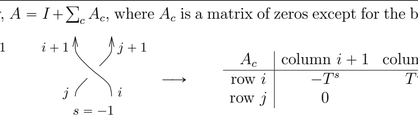

FIGURE 4.1. The modified Green function $\tilde g_{ab}$ is invariant under Reidemeister moves performed away from where it is measured.

Lemma 7. *Inserting a null vertex does not change $\tilde g_{ab}$ provided it is inserted away from the points a and b.*[4]

Proof. Let D be an upright knot diagram having an edge labelled i and let D' be obtained from it by adding a null vertex within edge i, naming the two resulting half-edges j and k (in order). Let $g_{\alpha\beta}$ be the Green function for D, and similarly, $g'_{\alpha\beta}$ for D'. We claim that

$$g'_{\alpha\beta} = \begin{cases} g_{ii} & g_{ii} & g_{i\beta} & \text{if } \alpha = j \\ g_{ii}-1 & g_{ii} & g_{i\beta} & \text{if } \alpha = k \\ g_{\alpha i} & g_{\alpha i} & g_{\alpha\beta} & \text{if } \alpha\notin\{j,k\} \end{cases} \qquad \text{(columns: if } \beta = j \text{, if } \beta = k \text{, if } \beta\notin\{j,k\}\text{)}$$

Indeed, all we have to do is to verify that the above-defined $g'_{\alpha\beta}$ satisfies all the g-rules (8)∪(11), and that is easy. The lemma now follows easily from the definition of $\tilde g'$ in Equation (10). □

Remark 8. The statement of our Main Theorem, Theorem 1, does not change in the presence of null vertices: There are no "F" terms for those, and their only effect on the definition of Θ in Equation (6) is to change the edge labels that appear within c, c_1, and c_2, and within the F_3 sum.

The following theorem was not named in [BV1] yet it was stated there as the first part of the first proof of [BV1, Theorem 1].

Theorem 9. *The variant Green function $\tilde g_{ab}$ is a "relative invariant", meaning that once points a and b are fixed within a knot diagram D, the value of $\tilde g_{ab}$ does not change if Reidemeister moves are performed* away *from the points a and b (an illustration appears in Figure 4.1). It follows that the same is also true for $\tilde g_{\nu ab}$ for $\nu = 1,2,3$.*

We note that $\tilde g_{ab}$ is nearly the same as $g_{\alpha\beta}$, if a is on α and b is on β. So Theorem 9 also says that $g_{\alpha\beta}$ is invariant under Reidemeister moves away from α and β, except for edge-renumbering issues and ±1 contributions that arise if α and β correspond to edges that get merged or broken by the Reidemeister moves.

The proof of Theorem 9 is perhaps best understood in terms of the traffic function of Discussion 3: One simply needs to verify that for each of the Reidemeister moves, traffic entering the tangle diagram for the left hand side of the move exits it in the same manner as traffic entering the tangle diagram for the right hand side of the move, and each of these verifications, as explained in [BV1, BN4, BN7], is very easy. Yet that proof is a bit

[4]This statement does not make sense for $g_{\alpha\beta}$, as inserting a null vertex changes the dimensions of the matrix $G = (g_{\alpha\beta})$.

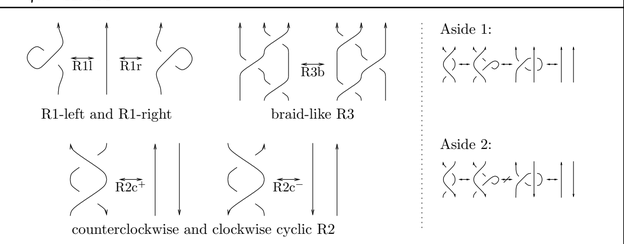

FIGURE 4.2. A generating set of oriented Reidemeister moves as in [Po2, Figure 6]. Aside 1: the braid-like R2b is not needed. Aside 2: yet R2b cannot replace R2c$^\pm$ because in the would-be proof, an unpostulated form of R3 is used (which in itself follows from R2c$^\pm$).

informal, so we opt here to give a fully formal proof along the lines of the first halves of [BV1, Propositions 7-9].

Proof of Theorem 9. We need to know how the Green function $g_{\alpha\beta}$ changes under the orientation-sensitive Reidemeister moves of Figure 4.2 (note that the $g_{\alpha\beta}$ do not see the rotation numbers and don't care if a knot diagram is upright in the sense of Figure 2.1.

We start with R3b. Below are the two sides of the move, along with the g-rules of type (8) corresponding to the crossings within, written with the assumption that β isn't in $\{i^+,j^+,k^+\}$, so several of the Kronecker deltas can be ignored. We use g for the Green function at the left-hand side of R3b, and g' for the right-hand side:

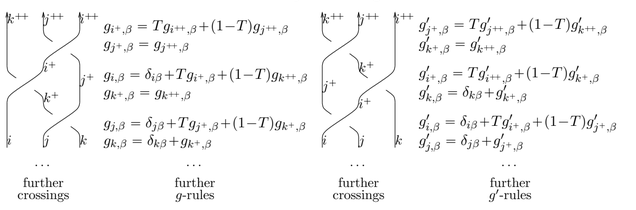
k^{++}
j^{++}
i^{++}
$g_{i^+,\beta} = Tg_{i^{++},\beta} + (1-T)g_{j^{++},\beta}$
$g_{j^+,\beta} = g_{j^{++},\beta}$
i^+
j^+
k^+
$g_{i,\beta} = \delta_{i\beta} + Tg_{i^+,\beta} + (1-T)g_{k^{++},\beta}$
$g_{k^+,\beta} = g_{k^{++},\beta}$
$g_{j,\beta} = \delta_{j\beta} + Tg_{j^+,\beta} + (1-T)g_{k^+,\beta}$
$g_{k,\beta} = \delta_{k\beta} + g_{k^+,\beta}$
i
j
k
...
further crossings
...
further g-rules
k^{++}
j^{++}
i^{++}
$g'_{j^+,\beta} = Tg'_{j^{++},\beta} + (1-T)g'_{k^{++},\beta}$
$g'_{k^+,\beta} = g'_{k^{++},\beta}$

```
Xl = {{1, j, k}, {1, i, k^+}, {1, i^+, j^+}};
Xr = {{1, i, j}, {1, i^+, k}, {1, j^+, k^+}};
Simplify[ESum[Append[Xl, {s, m, n}]] == ESum[Append[Xr, {s, m, n}]]]
```

```
True
```

12

Proposition 13. *The quantity θ_0 is invariant under the upright R2c$^+$ and R2c$^-$.*

Proof. For R2c$^+$ we follow the same logic as in the proof of Proposition 11, as simplified by Remark 12. We start with the figure that replaces Figure 4.4 (note the null vertices in D^r and their minimal effect as in Lemma 7 and Remark 8):

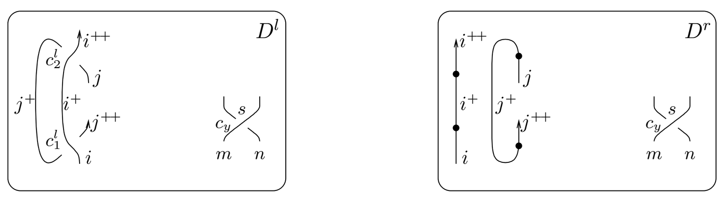

As in Remark 12, we let E^l and E^r be the sums corresponding to the diagrams D^l and D^r above:

$$E^l = \sum_{c\in\{c_1^l,c_2^l,c_y\}} F_1^l(c) + \sum_{c_0,c_1\in\{c_1^l,c_2^l,c_y\}} F_2^l(c_0,c_1) + F_3^l(j^+)|_{\varphi_{j^+}=1}, \quad E^r = F_1^r(c_y) + F_2^r(c_y,c_y) + F_3^r(j^+)|_{\varphi_{j^+}=1}.$$

We need to show that $E^l = E^r$ after all relevant g-rules are applied to both sides.

To compute these E sums we first have to extend the ESum routine to accept also a list R of pairs (φ, k) of the form (rotation number, edge label):

```
ESum[X_, R_] :=
  (Sum[F1[c], {c, X}] + Sum[F2[c0, c1], {c0, X}, {c1, X}] + Sum[F3 @@ r, {r, R}]) //.
    gRules @@ X;
```

We then compute E^l (and apply the relevant g-rules) by calling ESum with crossings $(-1, i, j^+)$, $(1, i^+, j)$, and (s, m, n), and a rotation number of 1 on edge j^+:

```
El = Simplify[ESum[{{-1, i, j^+}, {1, i^+, j}, {s, m, n}}, {{1, j^+}}]];
Short[El, 5]
```

```
-1/(2 (-1 + T2^s)) (1 + s + 2 s (T1 T2)^s g_{3,m^+,m} + <<11>> + 2 g_{3,(j^+)^+,j} -
   T2^s (1 + s - 2 s g_{1,n^+,m} g_{2,n^+,m} + <<29>> + 2 s g_{2,m^+,m} (1 + g_{3,n^+,n}) + 2 g_{3,(j^+)^+,j}))
```

The computation of E^r is simpler, as it only involves the generic (s,m,n) and the rotation $(1, j^+)$. We implement the g-rules for null vertices as in Equations (11) and (12), compute E^r, and then compare E^l with E^r to conclude the invariance under R2c$^+$:

```
gRules[j_] := {g_{ν_,j,β_} :> δ_{j,β} + g_{ν,j^+,β}, g_{ν_,α_,j^+} :> δ_{α,j^+} + g_{ν,α,j}}
```

```
Er = ESum[{{s, m, n}}, {{1, j^+}}] //. (Union @@ gRules /@ {i, i^+, j, j^+});
Simplify[El == Er]
```

```
True
```

For R2c$^-$ we allow ourselves to be even more concise:

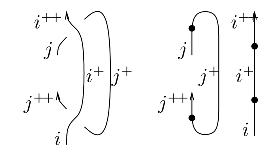

```
El = ESum[{{1, i, j^+}, {-1, i^+, j}, {s, m, n}}, {{-1, j^+}}];
Er = ESum[{{s, m, n}}, {{-1, j^+}}] //.
    (Union @@ gRules /@ {i, i^+, j, j^+});
Simplify[Er == El]
```

```
True
```

13

Proposition 14. *The quantity θ_0 is invariant under R1l and R1r.*

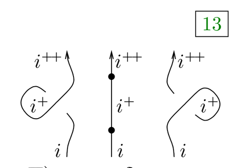

Proof. We aim to use the same approach and conventions as in the previous two proofs but hit a minor snag. The g-rules for R1l include

$$g_{i^+\beta} = \delta_{i^+\beta} + Tg_{i^{++},\beta} + (1-T)g_{i^+,\beta} \qquad \text{and} \qquad g_{\alpha,i^+} = g_{\alpha i} + (1-T)g_{\alpha i^+} + \delta_{\alpha,i^+},$$

and if these are implemented as simple left to right replacement rules, they lead to infinite recursion. Fortunately, these rules can be rewritten in the form

$$g_{i^+\beta} = T^{-1}\delta_{i^+\beta} + g_{i^{++},\beta} \qquad \text{and} \qquad g_{\alpha,i^+} = T^{-1}g_{\alpha i} + T^{-1}\delta_{\alpha,i^+},$$

which makes perfectly valid replacement rules. We thus redefine:

```
gRules[{1, i^+, i}] = {g_{ν_,i,β_} :> g_{ν,i^+,β} + δ_{i,β}, g_{ν_,i^+,β_} :> g_{ν,(i^+)^+,β} + T_ν^-1 δ_{i^+,β},
   g_{ν_,α_,(i^+)^+} :> T_ν g_{ν,α,i^+} + δ_{α,(i^+)^+}, g_{ν_,α_,i^+} :> T_ν^-1 g_{ν,α,i} + T_ν^-1 δ_{α,i^+}};
```

The same issue does not arise for R1r (!), and thus the following lines conclude the proof:

```
El = ESum[{{1, i^+, i}, {s, m, n}}, {{1, i^+}}];
Em = ESum[{{s, m, n}}];
Er = ESum[{{1, i, i^+}, {s, m, n}}, {{-1, i^+}}];
Simplify[El == Em == Er]
```

```
True
```

14

Proposition 15. *The quantity θ_0 is invariant under Sw.*

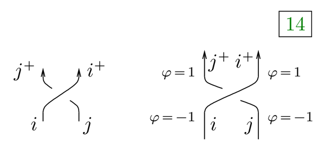

Proof. This one is routine:

```
El = ESum[{{1, i, j}, {s, m, n}}];
Er = ESum[{{1, i, j}, {s, m, n}}, {{-1, i}, {-1, j}, {1, i^+}, {1, j^+}}];
Simplify[El == Er]
```

```
True
```

15

Proposition 16. *The quantity θ_0 is invariant under NV.*

Proof. Indeed, F_3 is linear in φ. □

We are now ready to complete the proof of the first part of the Main Theorem.

Proof of Invariance. The invariance statement in the Main Theorem, Theorem 1, now follows from the invariance of the Alexander polynomial and from Propositions 10, 11, 13, 14, 15, and 16. □

4.2. **Proof of Polynomiality.** We already know (see Comment 2) that the only obstruction to the polynomiality of θ comes from the explicit denominators in Equations (3) and (4). These denominators are $(T_2-1)^{-1}$ (if $s, s_1 = 1$) or $(T_2^{-1}-1)^{-1} = -T_2(T_2-1)^{-1}$ (if $s, s_1 = -1$). So it is enough that we show that the residue R of θ at $T_2 = 1$ vanishes, and this residue comes solely from the residues of F_1 and F_2 at $T_2 = 1$. Thus R is the knot invariant coming from the same procedure as θ, only replacing F_1, F_2, and F_3 by their residues R_1, R_2 and R_3 at $T_2 = 1$. These residues are easily seen to be

$$R_1(c) = (T^s - 1)g_{ji}\left(g_{ii} + 2(T^s-1)g_{ji} - g_{jj}\right),$$

$$R_2(c_0,c_1) = (T^{s_0}-1)(T^{s_1}-1)g_{j_0i_1}g_{j_1i_0}\left(\chi_{i_1\leqslant i_0} - \chi_{i_1\leqslant i_0} - \chi_{j_1\leqslant i_0} + \chi_{j_1\leqslant j_0}\right),$$

and $R_3 = 0$, where we have simplified these formulas by making the following observations:

- R depends only on T_1 which we rename to be T.
- At $T_2 = 1$, $g_{3\alpha\beta} = g_{1\alpha\beta} = g_{\alpha\beta}$.
- At $T_2 = 1$, by a simple calculation of the matrices A and G and/or using the traffic interpretation of Comment 3, $g_{2\alpha\beta}$ is the indicator function $\chi_{\alpha\leqslant\beta}$ of the inequality $\alpha \leqslant \beta$, which is 1 if the inequality holds and 0 otherwise.

An explicit calculation for some specific knots shows that the sums corresponding to R_1 and to R_2 do not vanish individually; instead, they cancel each other. So we'd better find a technique that relates a double sum to a single sum. That's the content of the following lemma:

Lemma 17. *If there is a function $f(c_0,\gamma)$ that depends on a crossing c_0 and an additional edge label γ such that $(Bf)(c_0) \coloneqq f(c_0, 2n+1) - f(c_0, 1) = 0$ and such that for any additional crossing $c_1 = (s_1, i_1, j_1)$ we have that*

$$(\partial_{c_1}f)(c_0,c_1) \coloneqq f(c_0,i_1^+) + f(c_0,j_1^+) - f(c_0,i_1) - f(c_0,j_1) = R_2(c_0,c_1) + \delta_{c_0,c_1}R_1(c_0), \quad (19)$$

then the invariant R vanishes.

Proof. Indeed, using the above equation and then telescopic summation over c_1 and the vanishing of Bf,

$$R = \sum_{c_0,c_1} R_2(c_0,c_1) + \sum_c R_1(c) = \sum_{c_0,c_1}(\partial_{c_1}f)(c_0,c_1) = \sum_{c_0}(Bf)(c_0) = 0.$$

□

We can now complete the proof of the second part of the Main Theorem.

Proof of Polynomiality. Take $f(c_0,\gamma) \coloneqq (T^{s_0}-1)g_{\gamma i_0}g_{j_0^+\gamma}(\chi_{\gamma\leqslant i_0} - \chi_{\gamma\leqslant j_0})$. Use the easily proven facts that $g_{2n+1,i_0} = 0 = g_{j_0^+1}$ to show that $Bf = 0$ and then use g-rules to verify Equation (19). Now using Lemma 17 we have that $R = 0$ and therefore θ is a Laurent polynomial. The only non-integrality for the coefficients of θ may arise from the $s/2$ term in Equation (3) and from the $-\varphi_k/2$ terms in Equation (5). These add up to $(w(D) - \varphi(D)/2$, using the notation of Equation (2). But $w(D) - \varphi(D)$ is always an even number as it is 0 for the long unknot ↑ and its parity is unchanged by crossing changes and by the moves of Figure 4.3. □

An implementation and a verification of the assertions made in this section is at [BV3, Polynomiality.nb].

1	n	$\leqslant 10$	$\leqslant 11$	$\leqslant 12$	$\leqslant 13$	$\leqslant 14$	$\leqslant 15$
2	knots	249	801	2,977	12,965	59,937	313,230
3	Δ	(38)	(250)	(1,204)	(7,326)	(39,741)	(236,326)
4	σ_{LT}	(108)	(356)	(1,525)	(7,736)	(40,101)	(230,592)
5	J	(7)	(70)	(482)	(3,434)	(21,250)	(138,591)
6	Kh	(6)	(65)	(452)	(3,226)	(19,754)	(127,261)
7	H	(2)	(31)	(222)	(1,839)	(11,251)	(73,892)
8	*Vol*	(∼6)	(∼25)	(∼113)	(∼1,012)	(∼6,353)	(∼43,607)
9	(Kh, H, Vol)	(∼0)	(∼14)	(∼84)	(∼911)	(∼5,917)	(∼41,434)
10	(Δ, ρ_1)	(0)	(14)	(95)	(959)	(6,253)	(42,914)
11	(Δ, ρ_1, ρ_2)	(0)	(14)	(84)	(911)	(5,926)	(41,469)
12	$(\rho_1, \rho_2, Kh, H, Vol)$	(0)	(∼14)	(∼84)	(∼911)	(∼5,916)	(∼41,432)
13	Θ	(0)	(3)	(19)	(194)	(1,118)	(6,758)
14	(Θ, ρ_2)	(0)	(3)	(10)	(169)	(982)	(6,341)
15	(Θ, σ_{LT})	(0)	(3)	(19)	(194)	(1,118)	(6,758)
16	(Θ, Kh)	(0)	(3)	(18)	(185)	(1,062)	(6,555)
17	(Θ, H)	(0)	(3)	(18)	(185)	(1,064)	(6,563)
18	(Θ, Vol)	(0)	(∼3)	(∼10)	(∼169)	(∼973)	(∼6,308)
19	$(\Theta, \rho_2, Kh, H, Vol)$	(0)	(∼3)	(∼10)	(∼169)	(∼972)	(∼6,304)

TABLE 5.1. The separation powers of some knot invariants and combinations of knot invariants (in lines 3–19, smaller numbers are better). The data in this table was assembled by [BV3, Stats.nb].

5. Strong and Meaningful

5.1. **Strong.** To illustrate the strength of Θ, Table 5.1 summarizes the separation powers of Θ and of some common knot invariants and combinations of those knot invariants on prime knots with up to 15 crossings (up to reflections and reversals).

In line 2 of the table we list the total number of tabulated knots with up to n crossings. For example, there are 313,230 prime knots up to reflections and reversals with at most 15 crossings. In the following lines we list the *separation deficits* on these knots, for different invariants or combinations of invariants. For example, in line 3 we can see that on knots with up to 10 crossings, the Alexander polynomial Δ has a separation deficit of 38: meaning, that it attains $249 - 38 = 211$ distinct values on the 249 knots with up to 10 crossings. For deficits, the smaller the better![5] Thus the deficit of 236,326 for Δ at $n \leqslant 15$ means that the Alexander polynomial is a rather weak invariant, in as much as separation power is concerned.

In line 4 we shows the deficits for the Levine-Tristram signature σ_{LT} [Le, Tr, Co] as computed by the program in [BN5]. We were surprised to find that for knots with up to 15 crossings these deficits are smaller than those of Δ.

Line 5 shows the deficits for the Jones polynomial J. It is better than Δ, and better than Δ and σ_{LT} taken together (deficits not shown) but still rather weak. Line 6 shows the

[5]This is not a political statement.

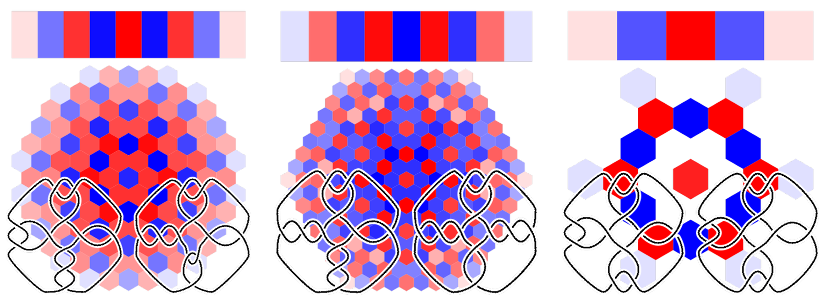

FIGURE 5.1. The three pairs responsible for the deficit of 3 in the column $n \leqslant 11$ of line 13 of Table 5.1. They are $(11_{a44}, 11_{a47})$, $(11_{a57}, 11_{a231})$, and $(11_{n73}, 11_{n74})$, and each pair is a pair of mutant Montesinos knots (though Θ sometimes does separate mutant pairs, as was shown in Section 3.2).

deficits for Khovanov homology Kh. They are only a bit lower than those of J. On line 7, the HOMFLY-PT polynomial H is noticeably better.

On line 8 we consider the hyperbolic volume *Vol* of the knot complement, as computed by SnapPy [CDGW]. We computed volumes using SnapPy's `high_precision` flag, which makes SnapPy compute to roughly 63 decimal digits, and then truncated the results to 58 decimal digits to account for possible round-off errors within the last few digits. But then we are unsure if we computed enough.... Hence the uncertainty symbols "∼" on some of the results here and in the other lines that contain *Vol*. This said, *Vol* seems to be the champion so far.

Line 9 is "everything so far, taken together". Note that Kh dominates J and H dominates both Δ and J, so there's no point adding Δ and/or J into the mix. We note that adding σ_{LT} to the triple (Kh, H, Vol), or even to the pair (Kh, Vol), does not improve the results; namely, for knots with up to 15 crossings the pair (Kh, Vol) dominates σ_{LT}, even though each of Kh and *Vol* does not dominate σ_{LT} and the discrepancies start already at 11 crossings. We don't know if this means anything.

On line 10, the Rozansky-Overbay invariant ρ_1 [Roz1, Roz2, Roz3, Ov], also discussed by us in [BV1], does somewhat better. Note that the computation of Δ is a part of the computation of ρ_1, so we always take them together. In line 11 we add ρ_2 [BN4] to make the results yet a bit better.

Line 12 is "everything before Θ".

Line 13 makes our case that Θ is strong — the deficit here, for knots with up to 15 crossings, is about a sixth of the deficit in line 12! For the interested, Figure 5.1 shows the 3 pairs that create the deficit in the column $n \leqslant 11$ of this line.

Line 14 reinforces our case by just a bit: note that it makes sense to bundle ρ_2 along with Θ, for their computations are very similar. Note also that Conjecture 24 below means that it is pointless to consider (Θ, ρ_1).

Line 15 shows that for knots with up to 15 crossings, Θ dominates σ_{LT}. We don't know if this persists.

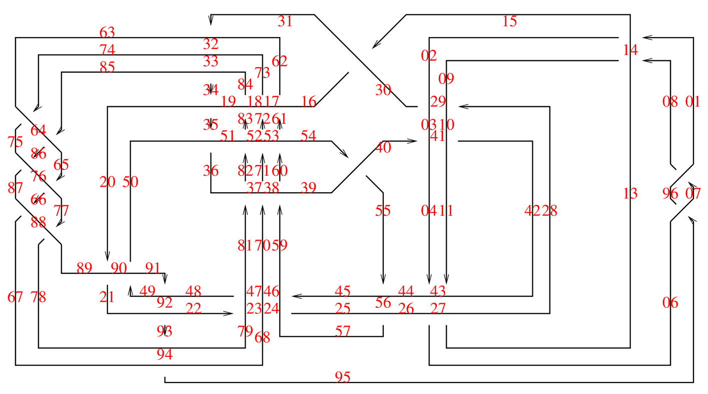

FIGURE 5.2. The 48-crossing Gompf-Scharlemann-Thompson GST_{48} knot [GST].

Lines 16 through 18 show that at crossing number $\leqslant 15$ and in the presence of Θ, and especially in the presence of both Θ and ρ_2, it is pointless to also consider H or Kh, and only mildly useful to also consider *Vol*. Line 19 shows that once *Vol* has been added to Θ, the other invariants contribute almost nothing.

We note that of all the invariants considered above, the only one known to (sometimes) detect knot mutation is Θ (see Section 3.2).

We also note that the V_n polynomials of Garoufalidis and Kashaev [GK], and in particular V_2 [GL] share many properties with Θ and are stronger than Θ on knots with up to 15 crossings. But they are not nearly as computable on large knots. It would be very interesting to explore the relationship between the V_n's and Θ.

5.2. **Meaningful.** Many knot polynomials have some separation power, some more and some less, yet they seem to "see" almost no other topological properties of knots. The greatest exception is the Alexander polynomial, which despite having rather weak separation powers, gives a genus bound, a fiberedness condition, and a ribbon condition. The definition of θ is in some sense "near" the definition of Δ, and one may hope that θ will share some of the good topological properties of Δ.

5.2.1. *The Knot Genus.* With significant computational and theoretical evidence (see also Discussion 26 and Comment 29 below) we believe the following to be true:

Conjecture 18. *Let K be a knot and $g(K)$ the genus of K. Then $\deg_{T_1}\theta(K) \leqslant 2g(K)$.*

Using the available genus data in KnotInfo [LM] we have verified this conjecture for all knots with up to 13 crossings (see [BV3, KnotGenus.nb]). The example of the Conway knot and the Kinoshita-Terasaka knot in Section 3.2 shows that the bound in Conjecture 18 can be stronger than the bound $\deg_T\Delta(K) \leqslant g(K)$ coming from the Alexander polynomial. Another such example is the 48-crossing Gompf-Scharlemann-Thompson GST_{48} knot [GST] of Figure 5.2. Here's the relevant computation, with $X_{14,1}$ (say) meaning "the crossing $(1, 14, 1)$" and $\bar{X}_{2,29}$ (say) meaning "$(-1, 2, 29)$":

```
GST48 = EPD[X_{14,1}, X̄_{2,29}, X_{3,40}, X_{43,4}, X̄_{26,5},
    X_{6,95}, X_{96,7}, X_{13,8}, X̄_{9,28}, X_{10,41}, X_{42,11}, X̄_{27,12},
    X_{30,15}, X̄_{16,61}, X̄_{17,72}, X̄_{18,83}, X_{19,34}, X̄_{89,20},
    X̄_{21,92}, X̄_{79,22}, X̄_{68,23}, X̄_{57,24}, X̄_{25,56}, X̄_{62,31},
    X_{73,32}, X̄_{84,33}, X̄_{50,35}, X_{36,81}, X̄_{37,70}, X̄_{38,59},
    X̄_{39,54}, X_{44,55}, X̄_{58,45}, X_{69,46}, X̄_{80,47}, X_{48,91},
    X_{90,49}, X̄_{51,82}, X̄_{52,71}, X_{53,60}, X̄_{63,74}, X̄_{64,85},
    X̄_{76,65}, X̄_{87,66}, X̄_{67,94}, X̄_{75,86}, X̄_{88,77}, X̄_{78,93}];
AbsoluteTiming@
  PolyPlot[{Δ48, θ48} = Θ[GST48],
    ImageSize → Small]
```

{14.5823,

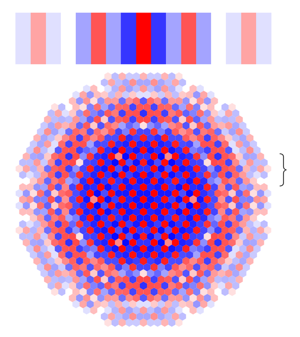

}

```
{Exponent[Δ48, T], ⌈Exponent[θ48, T1] / 2⌉}
```

```
{8, 10}
```

Thus θ gives a better lower bound on the genus of GST_{48}, 10, then the lower bound coming from Δ, which is 8. Seeing that GST_{48} may be a counter-example to the ribbon-slice conjecture [GST], we are happy to have learned more about it. Also see Dream 38 below.

The hexagonal QR code of large knots is often a clear hexagon (e.g. Figure 1.4), but the hexagonal QR code of GST_{48}, displayed above, is rounded at the corners. We don't know if this is telling us anything about topological properties of GST_{48}.

5.2.2. *Fibered Knots.* Upon inspecting the values of Θ on the Rolfsen table, Figure 1.1, we noticed that often (but not always) the bar code shows the exact same colour sequence as the top row of the QR code, or exactly its opposite. This and some experimentation lead us to the following conjecture, for which we do not have theoretical support. See a similar result on the ADO invariant at [LV].

Conjecture 19. *If K is a fibered knot and d is the degree of $\Delta(K)$ (the highest power of T), then the coefficient of T_2^{2d} in $\theta(K)$, which is a polynomial in T_1, is an integer multiple of $T_1^d\Delta(K)|_{T\to T_1}$. See examples in Figure 5.3, where the integer factor is denoted $s(K)$.*

Using the available fiberedness data in KnotInfo [LM] we found that the condition in this conjecture holds for all 5,397 fibered knots with up to 13 crossings, while it fails on all but 48 of the 7,568 non-fibered knots with up to 13 crossings. See [BV3, FiberedKnots.nb].

We note that if K is fibered then degree d of $\Delta(K)$ is the genus of K, and $\Delta(K)$ is monic, meaning that the coefficient of T^d in $\Delta(K)$ is ± 1 (see [Rol, Section 10H]). The latter condition is an often-used fast-to-compute criterion for a knot to be fibered.

If Conjecture 19 is true then the condition in it is another fast-to-compute criterion for a knot to be fibered, and this criterion is sometimes stronger than the Alexander condition. For example, both the Conway and the Kinoshita-Terasaka knots are not fibered yet their Alexander polynomial is 1, which is monic. In both cases the coefficient of T_2^0 in θ is not an integer multiple of 1 (see Section 3.2), so the condition in Conjecture 19 would detect that these two knots are not fibered.

6. Stories, Conjectures, and Dreams

There is a storyteller in each of us, who wants to tell a coherent story, with a beginning, a middle, and an end. Unfortunately of us, the Θ story isn't that neat. Calling the content

FIGURE 5.3. The invariant Θ of the fibered knot 12_{n242}, also known as the $(-2, 3, 7)$ pretzel knot, and of the fibered knot 7_7. For the first, $s(K) > 0$ and the bar code visibly matches with the top row of the QR code (though our screens and printers and eyes may not be good enough to detect minor shading differences, so a visual inspection may not be enough). For the second, twice the degree of Δ is visibly greater than the degree of θ, so $s(K) = 0$.

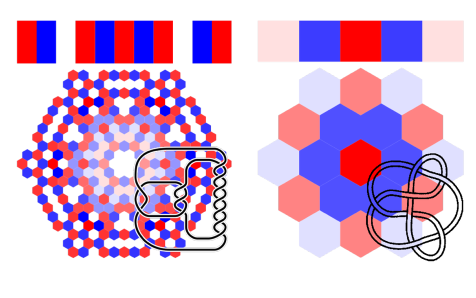

FIGURE 6.1. A long version of the rotational virtual knot KS from [Kau3]. It has $X = \{(-1,1,6), (-1,2,4), (1,9,3), (-1,7,5), (1,10,8)\}$ and $\varphi = (-1,0,0,1,0,-1,0,0,1,0,0)$.

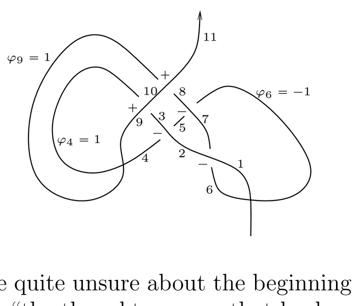

of the first few sections of this paper "the middle", we are quite unsure about the beginning and the end. The "beginning" can be construed to mean "the thought process that lead us here". But that process was too long and roundabout to be given in full here (though much of it can be gleaned by reading this section). What's worse, we believe that ultimately, our peculiar thought process will be replaced by much more solid foundations and motivations, perhaps along the lines of Dreams 35 and 36. But this solid foundation is not available yet, even if we are working hard to expose it. As for the end of the story, it is clearly in the future.

Hence this section is a bit sketchy and disorganized. Those facts that we already know, those conjectures we believe in, and the dreams we dream, are here in some random order. But the narrative is lacking.

Many of the statements below continue a theme from Section 5.2, that θ shares many of the properties of Δ, and sometimes sharpens them.

Conjecture 20. *θ has hexagonal symmetry. That is, for any knot K, $\theta(K)$ is invariant under the substitutions $(T_1 \to T_1, T_2 \to T_1^{-1}T_2^{-1})$ ("the QR code is invariant under reflection about a horizontal line"), and $(T_1 \to T_1T_2, T_2 \to T_2^{-1})$ ("the QR code is invariant under reflection about the line of slope 30°").*

The Alexander polynomial Δ is invariant under a simpler symmetry, $T \to T^{-1}$. It is rather difficult to deduce the symmetry of Δ from the formula in this paper, Equation (2) (though it is possible; once notational differences are overcome, the proof is e.g. in [CF, Chapter IX]). Instead, the standard proof of the symmetry of Δ uses the Seifert surface formula for Δ (e.g. [Li, Chapter 6]). We expect that Conjecture 20 will be proven as soon as a Seifert formula is found for θ. See Dream 35 below.

A *rotational virtual knot* is a virtual knot diagram [Kau2] whose edges[6] are marked with "rotation numbers" φ_k, modulo the same moves as in Figure 4.3.[7] Clearly, Θ extends to long rotational virtual knots, and the proof of the Main Theorem, Theorem 1, extends nearly verbatim[8]. Yet as shown below, on the long rotational virtual knot KS of Figure 6.1 (and indeed, on almost any other long rotational virtual knot which is not a classical knot), the hexagonal symmetry of θ fails. So something non-local must happen within any proof of Conjecture 20.

```
KS = {{{-1, 1, 6}, {-1, 2, 4}, {1, 9, 3}, {-1, 7, 5}, {1, 10, 8}},
    {0, 0, 0, 1, 0, -1, 0, 0, 1, 0, 0}};
PolyPlot[Θ[KS], ImageSize → Tiny]
```

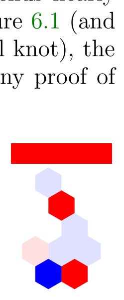

Conjecture 21. *If $\bar{K}$ denotes the mirror image of a knot K, then $\theta(\bar{K}) = -\theta(K)$.*

Conjecture 22. *If $-K$ denotes the reverse of a knot K (namely, K taken with the opposite orientation), then $\theta(-K) = \theta(K)$.*

Fact 23. *$\theta_0(K)$ is additive under the connected sum operation of knots: $\theta_0(K_l \# K_r) = \theta_0(K_l) + \theta_0(K_r)$. Equivalently, using the known multiplicativity of Δ,*

$$\theta(K_l\#K_r) = \theta(K_l)\Delta_1(K_r)\Delta_2(K_r)\Delta_3(K_r) + \theta(K_r)\Delta_1(K_l)\Delta_2(K_l)\Delta_3(K_l).$$

Oddly, Fact 23 is easier to prove than Conjectures 21 and 22:

Proof Sketch. The F_1 and F_3 summations in Equation (6) are clearly additive, and so is the part of the F_2 summation in which c_0 and c_1 fall within the same component. It remains to consider the case where c_0 and c_1 fall within different components. But in that case, the factor $g_{1j_1i_0}g_{3j_0i_1}$ within the definition of F_2 in (4) vanishes because cars only drive forward, and either $g_{1j_1i_0}$ or $g_{3j_0i_1}$ measures traffic going backwards. □

Conjecture 24. *θ dominates the Rozansky-Overbay invariant ρ_1 [Roz1, Roz2, Roz3, Ov], also discussed by us in [BV1]. In fact, $\rho_1 = -\theta|_{T_1\to T, T_2\to 1}$.*

Conjecture 25. *θ is equal to the "two-loop polynomial" studied extensively by Ohtsuki [Oh2], continuing Rozansky, Garoufalidis, and Kricker [GR, Roz1, Roz2, Roz3, Kr].*

Discussion 26. People who are already familiar with "the loop expansion" may consider the above conjecture an "explanation" of θ. We differ. An elementary construction ought to have a simple explanation, and the loop expansion is too complicated to be that.

Be it as it may, Ohtsuki [Oh2] shows that Conjecture 25 implies Conjectures 18, 20, 21, and 22 as well as Fact 23. Conjecture 25 would also predict the behaviour of θ under Whitehead doubles as in [Gar] and under cabling operations as in [Oh3]. 26

Next, let us briefly sketch some key points from [BN2, BV2], where we explain how to obtain poly-time computable knot invariants from certain Lie algebraic constructions.

[6]Ignoring "virtual crossings". See [BDV, Section 4].
[7]This definition is slightly different than the original in [Kau3] but the equivalence is easy to show.
[8]The only exception is that some of the coefficients of θ may be half integers, as $w(D) - \varphi(D)$ may be odd for a rotational virtual knot diagram.

Discussion 27. Let $\mathfrak{g}$ be a semi-simple Lie algebra, let $\mathfrak{b}$ be its upper Borel subalgebra, and let $\mathfrak{h}$ be its Cartan subalgebra. Then $\mathfrak{b}$ has a Lie bracket β and, as the dual of the lower Borel subalgebra, it also has a cobracket δ. It turns out that $\mathfrak{g}$ can be recovered from the triple $(\mathfrak{b}, \beta, \delta)$; in fact, $\mathfrak{g}^+ \coloneqq \mathfrak{g} \oplus \mathfrak{h} \simeq \mathcal{D}(\mathfrak{b}, \beta, \delta)$, where $\mathcal{D}$ denotes the Manin double construction[9]. We now set $\mathfrak{g}^+_\epsilon \coloneqq \mathcal{D}(\mathfrak{b}, \beta, \epsilon\delta)$, where ϵ is a formal "small" parameter. The family $\mathfrak{g}^+_\epsilon$ is a 1-parameter family of Lie algebras all defined on the same underlying vector space $\mathfrak{b} \oplus \mathfrak{b}^*$. If ϵ is invertible then $\mathfrak{g}^+_\epsilon$ is independent of ϵ and is always isomorphic to $\mathfrak{g}^+ = \mathfrak{g}^+_1$. Yet at $\epsilon = 0$, $\mathfrak{g}^+_0$ is solvable, and as the name "solvable" suggests, computations in $\mathfrak{g}^+_0$ can be "solved", meaning, can be carried out efficiently in closed form.

Hence in [BN2, BV2], mostly in the case where $\mathfrak{g} = sl_2$, we use standard techniques to quantize the universal enveloping algebra $\mathcal{U}(\mathfrak{g}^+_\epsilon)$ and use it to define a "universal quantum invariant" $Z^{\mathfrak{g}}_\epsilon$ (in the sense of [Law, Oh1]). We then expand $Z^{\mathfrak{g}}_\epsilon$ near where it's easy; namely, as a power series around $\epsilon = 0$. In the case of $\mathfrak{g} = sl_2$, and almost certainly in general, we write $Z^{\mathfrak{g}}_\epsilon = \rho^{\mathfrak{g}}_0 \exp\left(\sum_{d\geqslant 1}\rho^{\mathfrak{g}}_d\epsilon^d\right)$ and find that we can interpret the $\rho^{\mathfrak{g}}_d$ as polynomials in as many variables as the rank of $\mathfrak{g}$. It turns out that $\rho^{\mathfrak{g}}_0$ is always determined by the Alexander polynomial and the $\rho^{\mathfrak{g}}_d$ are always computable in polynomial time (with polynomials whose exponents and coefficients get worse as d grows bigger and $\mathfrak{g}$ gets more complicated).

Our papers and talks [BV1, BV2, BN4] carry out the above procedure in the case where $\mathfrak{g} = sl_2$, calling the resulting invariants ρ_d, for $d \geqslant 1$. They are the same as ρ_1 and ρ_2 of Section 5.1. 27

Following some preliminary work by Schaveling [Sch], in the summer of 2024 we've set out to find good formulas for $\rho_1^{sl_3}$. Tracing Discussion 27 seemed technically hard, so instead, we extracted from the procedure the "shape" of the formulas we could expect to get and, and then we found the invariant θ by the method of undetermined coefficients assisted by some difficult-to-formulate intuition (more in Comment 34 below). Thus our formulas for θ arose from our expectations for $\rho_1^{sl_3}$, and yet we have not proved that they are equal!

Conjecture 28. *Up to conventions and normalizations, $\theta = \rho_1^{sl_3}$.*

Comment 29. Using the techniques of [BN3, BV2] we expect to be able to prove a genus bound for $\rho_1^{sl_3}$, similar to the bound in Conjecture 18. Thus we expect that Conjecture 28 will imply Conjecture 18.

Discussion 30. People who are versed with Lie algebras and their quantizations may consider the above an "explanation" of θ, and may be looking forward to a more detailed exposition of $\rho^{\mathfrak{g}}_d$. We differ, for the same reasons as in Discussion 26. We expect the eventual "origin story" of θ to be simpler and more natural. 30

Discussion 31. Seeing that the coproduct of the quantized algebras of Discussion 27 correspond to strand doubling, and also noting Ohtsuki's [Oh3], we expect that there should be cabling and satellite formulas for all the invariants of the type $\rho^{\mathfrak{g}}_d$, and in particular for Θ. In particular, it should not be possible to increase the separation power of Θ by pre-composing it with cabling or satellite operations. 31

[9]We are unsure about naming. $\mathcal{D}$ is also known as "the Drinfeld double" construction for Lie bialgebras (as opposed to Hopf algebras). Yet when Drinfeld first refers to this construction in [Dr], in reference to Lie bialgebras, he repeatedly names it after Manin (under the less clear name "Manin triples"), yet without providing a reference. Our choice is to use "Manin double" when doubling Lie bialgebras and "Drinfeld double" when doubling a Hopf algebra, as we found no indication that Manin knew about the latter process.

Discussion 32. It is the basis of the theory of "Feynman diagrams", and hence it is extremely well known in the physics community, that perturbed Gaussian integrals, when convergent, can be computed (as asymptotic series) efficiently using "Feynman diagrams" (see e.g. [Po1]). Physicists use this routinely in infinite dimensions; yet the finite dimensional formulation can be sketched as follows:

$$\int_{\mathbb{R}^d} e^{Q+\epsilon P} \sim C\sum_{n\geqslant 0}\epsilon^n\sum_F \mathcal{E}(F), \quad (20)$$

where Q is a non-degenerate quadratic on $\mathbb{R}^d$, P is a "smaller" perturbation, C is some constant involving π's and the determinant of Q, the summation $\sum_F$ is over "Feynman diagrams" of complexity n, and $F \mapsto \mathcal{E}(F)$ is some procedure, which can be specified in full but we will not do it here, which assigns to every Feynman diagram F an algebraic sum which in itself depends only on the coefficients of P and the entries of the inverse of Q.

In fact, one may take the right-hand-side of Equation (20) to be the definition of the left-hand-side, especially if the left-hand-side is not convergent, or does not make sense for some other reason. Namely, one may set

$$\oint_{\mathbb{R}^d} e^{Q+\epsilon P} \coloneqq C\sum_{n\geqslant 0}\epsilon^n\sum_F \mathcal{E}(F). \quad (21)$$

The result is an integration theory defined on perturbed Gaussians in fully algebraic terms, and which shares some of the properties of "ordinary" integration, such as having a version of Fubini's theorem. In a sense, that's what physicists do: path integrals don't quite make sense, so instead they are defined using Feynman diagrams and the right-hand-side of Equation (21). Another example is the "Århus integral" of [BGRT], where the integral in itself is diagrammatic, as is the output of the integration procedure. 32

Fact 33. *There is a perturbed Gaussian formula for Θ. More precisely, one can assign a 6-dimensional Euclidean space $\mathbb{R}^6_e$ with coordinates $p_{1e}, p_{2e}, p_{3e}, x_{1e}, x_{2e}, x_{3e}$ to each edge e of a knot diagram D and then form $\mathbb{R}_{6E} \coloneqq \prod_e \mathbb{R}^6_e$, a space whose dimension is 6 times the number of edges in E. One can then form a "Lagrangian" $L_D = Q_D + \epsilon P_D$ by summing over all the crossings of D local contributions that involve only the variables associated with the four edges around each crossings, and adding a "correction" which is a sum over the edges e of D of terms that depend only on the rotation number of e and on the variables in $\mathbb{R}^6_e$, such that*

$$\oint_{\mathbb{R}_{6E}} e^{L_D} = \oint_{\mathbb{R}_{6E}} e^{Q_D+\epsilon P_D} = \frac{(2\pi)^{3|E|}}{\Delta_1\Delta_2\Delta_3}\exp(\epsilon\theta_0) + O(\epsilon^2),$$

and such that the Feynman diagram expansion of the left-hand-side of the above equation becomes precisely formula (6) for θ. See more about all this in [BN6].

Comment 34. In fact, Fact 33 is what we initially predicted based on Discussion 27, along with some further information about the "shape" of P_D. We used the method of undetermined coefficients to find precise formulas for P_D, and then the technique of Feynman diagrams to derive our main formula, Equation 6.

Dream 35. *There is a "Seifert formula" for Θ. More precisely, let K be a knot, let Σ be a Seifert surface for K, let $H \coloneqq H_1(\Sigma;\mathbb{R})$, and let $6H$ denote $H\oplus H\oplus H\oplus H\oplus H\oplus H$. Let Q_Σ denote 3 copies of the standard Seifert form on $H\oplus H$, taken with parameters T_1, T_2, and T_3; so Q_Σ is a quadratic on $6H$. We dream that there a "perturbation term" P_Σ, a polynomial function on $6H$ defined in terms of some low degree finite type invariants of various knotted graphs formed by representatives of classes in H (also taking account of their intersections), such that*

$$\oint_{6H} e^{L_\Sigma} = \oint_{6H} e^{Q_\Sigma+\epsilon P_\Sigma} = \frac{(2\pi)^{3\dim(H)}}{\Delta_1\Delta_2\Delta_3}\exp(\epsilon\theta_0) + O(\epsilon^2).$$

If this dream is true, it will probably prove Conjectures 18, 20, 21, and 22 much as the Seifert formula for Δ can be used to prove the genus bound provided by Δ and its basic symmetry properties.

We note the relationship between this dream and [Oh2, Theorem 4.4].

Dream 36. *All the invariants from Discussion 27 have Seifert formulas in the style of Dream 35. In fact, there ought to be a characterization of those Lagrangians L_Σ for which $\oint e^{L_\Sigma}$ is a knot invariant, and there may be a construction of all those Lagrangians which is intrinsic to topology and does not rely on the theory of Lie algebras.*

If a knot K is ribbon then for some g it has a Seifert surface Σ of genus g such that g of the generators of $H_1(\Sigma)$ can be represented by a g-component unlink (see the hint on the right, and see further details in [Kau1, Chapter VIII] or in [Ba, Section 3.4]). This implies that the Seifert matrix M of Σ has the form $\begin{pmatrix} 0 & A \\ A^* & B\end{pmatrix}$, which implies that the determinant of M, the Alexander polynomial Δ, satisfies the Fox-Milnor condition:

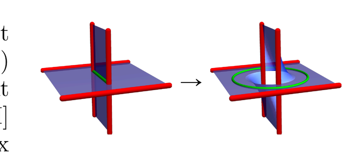

Theorem 37 (Fox and Milnor, [FM])**.** *If K is a ribbon knot, then there exists some polynomial $f(T)$ such that $\Delta = f(T)f(T^{-1})$.*

Dream 38. *Dream 35, along with the fact that half the homology of a Seifert surface of a ribbon knot can be represented by an unlink, will imply that θ takes a special form on ribbon knots, giving us stronger powers to detect knots that are not ribbon.*

Discussion 39. In this paper we concentrated on knots, yet at least partially, Θ can be generalized also to links. Indeed, the definitions in Section 2 and the proof in Section 4 go through provided the matrix A is invertible; namely, provided the Alexander polynomial Δ is non-zero (for knots, this is always the case), and provided we choose one component of the link to cut open.

The programs of Section 3 fail for minor reasons, and a fix is in [BV3, Theta4Links.nb]. Some results are in Figure 6.2. Preliminary testing using these programs suggests that the resulting invariant is independent of the choice of the cut component, but we did not prove that.

If $\Delta = 0$, one may contemplate replacing $G = A^{-1}$ by the adjugate matrix $\mathrm{adj}(A)$ of A (the matrix of codimension 1 minors, which satisfies $A\cdot\mathrm{adj}(A) = \det(A)I$).[10] Some preliminary testing is also in [BV3, Theta4Links.nb]. Yet if G is replaced with $\mathrm{adj}(A)$, its equivalence with the g-rules (Equations (8) and (9)) breaks, and so we have no proof of invariance. We may attempt to fix that in a future work, but it is not done yet.

[10]Similar "adjugate" reasoning shows that θ is always divisible by $\Delta^{(2)}(T_1)\Delta^{(2)}(T_2)\Delta^{(2)}(T_3)$, where $\Delta^{(2)}(T)$ is the second Alexander polynomial (e.g. [BZ, Definition 8.10]).

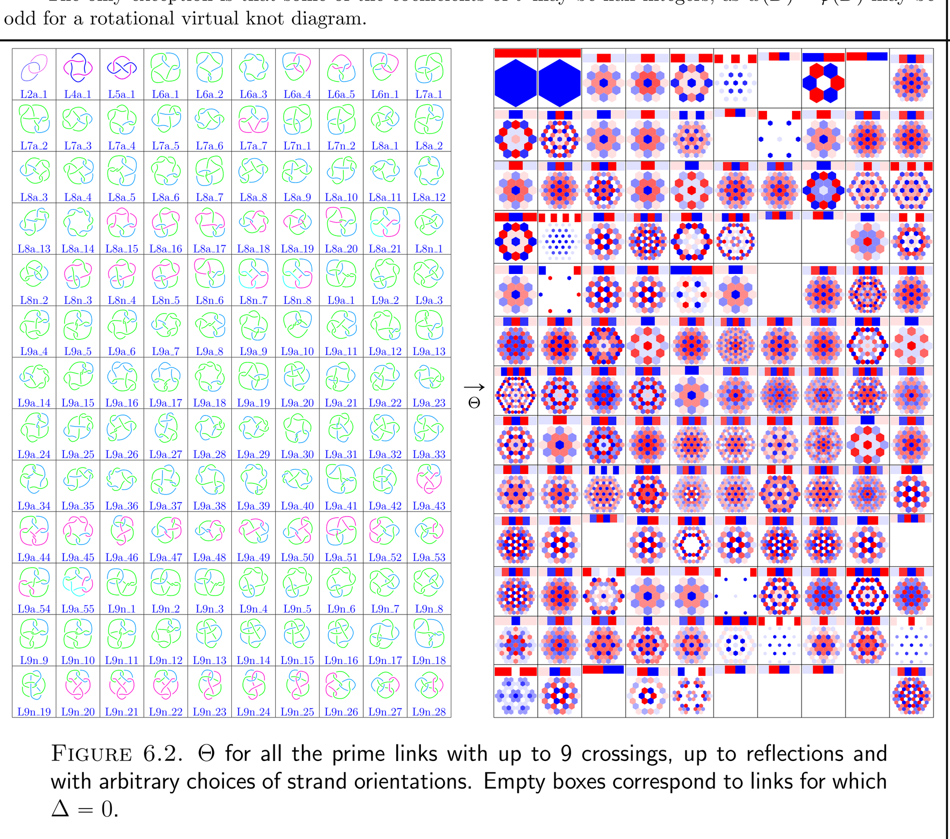

FIGURE 6.2. Θ for all the prime links with up to 9 crossings, up to reflections and with arbitrary choices of strand orientations. Empty boxes correspond to links for which $\Delta = 0$.

We note that the loop expansion of Conjecture 25 does not predict that Θ should extend to links. We also note that the solvable approximation technique of Discussion 27 does predict such an extension, and in fact, it predicts more: that much like the Gassner representation [Gas] and the multi-variable Alexander polynomial (e.g. [Kaw, Chapter 7]), there should be a multi-variable version of Θ which would be a polynomial in $2m$ variables when evaluated on an m-component link. We did not attempt to find explicit formulas for the multi-variable Θ. 39

Ever since Khovanov homology [Kh, BN1] it is almost mandatory to ask about anything, "does it categorify?". Θ is not exempt:

Question 40. Is there a categorification of θ? Is there a finite triply-graded chain complex whose Euler characteristic is θ and whose homology is invariant?

We note that θ is a neighbor of Δ (indeed they live together within Θ), and that Δ is categorified by knot Floer homology [OS, Ma, Ju]. Thus one may wonder if a categorification of θ will end up a neighbor of Floer knot homology. This applies even more to a possible categorication of $g_{\alpha\beta}$:

Question 41. Is there a categorification of $\Delta\cdot\tilde{g}_{ab}$? Is there a finite doubly-graded chain complex whose Euler characteristic is $\Delta\cdot\tilde{g}_{ab}$ and whose homology is a relative invariant in the sense of Theorem 9?

The latter seems likely: $\Delta\cdot\tilde{g}_{ab}$ is, after all, a minor of a matrix whose determinant is Δ.

7. Acknowledgement

We wish to thank Jorge Becerra and Stavros Garoufalidis for comments and suggestions. This work was partially supported by NSERC grants RGPIN-2018-04350 and RGPIN-2025-06718 and by the Chu Family Foundation (NYC).

References

[Al] J. W. Alexander, *Topological invariants of knots and links,* Trans. Amer. Math. Soc. **30** (1928) 275–306. See pp. 2.
[Ba] S. Bai, *Alexander Polynomials of Ribbon Knots and Virtual Knots,* arXiv:2103.07128. See pp. 31.
[BN1] D. Bar-Natan, *On Khovanov's Categorification of the Jones Polynomial,* Algebraic and Geometric Topology **2-16** (2002) 337–370, arXiv:math.GT/0201043. See pp. 32.
[BN2] D. Bar-Natan, *Everything around sl^ϵ_{2+} is DoPeGDO. So what?,* talk given in "Quantum Topology and Hyperbolic Geometry Conference", Da Nang, Vietnam, May 2019. Handout and video at ωεβ/DPG. See pp. 28, 29.
[BN3] D. Bar-Natan, *Algebraic Knot Theory,* talk given in Sydney, September 2019. Handout and video at ωεβ/AKT. See pp. 29.
[BN4] D. Bar-Natan, *Cars, Interchanges, Traffic Counters, and some Pretty Darned Good Knot Invariants,* talk given in Oaxaca, October 2022. Video and handout at http://drorbn.net/oa22. See pp. 14, 24, 29.
[BN5] D. Bar-Natan, *Shifted Partial Quadratics, their Pushforwards, and Signature Invariants for Tangles,* talk given in Geneva, December 2023. Video and handout at http://drorbn.net/ge23. See pp. 23.
[BN6] D. Bar-Natan, *Knot Invariants from Finite Dimensional Integration,* talks in Beijing (July 2024, http://drorbn.net/icbs24), Geneva (August 2024, http://drorbn.net/ge24) and Bonn (May 2025, http://drorbn.net/bo25). See pp. 6, 7, 30.
[BN7] D. Bar-Natan, *The Strongest Genuinely Computable Knot Invariant in 2024,* talk given in Toronto (October 2024, http://drorbn.net/to24). See pp. 6, 14.
[BDV] D. Bar-Natan, Z. Dancso and R. van der Veen, *Over then Under Tangles,* J. of Knot Theory and its Ramifications **32-8** (2023), arXiv:2007.09828. See pp. 28.
[BGRT] D. Bar-Natan, S. Garoufalidis, L. Rozansky, and D. P. Thurston, *The Århus integral of rational homology 3-spheres I–III,* Selecta Math., New Series **8** (2002) 315–339, arXiv:q-alg/9706004, **8** (2002) 341–371, arXiv:math.QA/9801049, **10** (2004) 305–324, arXiv:math.QA/9808013. See pp. 30.
[BV1] D. Bar-Natan and R. van der Veen, *A Perturbed-Alexander Invariant,* Quantum Topology **15** (2024) 449–472, arXiv:2206.12298. See pp. 6, 7, 11, 12, 14, 15, 24, 28, 29.
[BV2] D. Bar-Natan and R. van der Veen, *Perturbed Gaussian Generating Functions for Universal Knot Invariants,* arXiv:2109.02057. See pp. 28, 29.
[BV3] D. Bar-Natan and R. van der Veen, *A Fast, Strong, Topologically Meaningful, and Fun Knot Invariant,* (self-reference), paper and related files at http://drorbn.net/Theta. The arXiv:2509.18456 edition may be older. See pp. 4, 8, 11, 22, 23, 25, 26, 31.
[BVH] J. Becerra and K. van Helden, *Minimal Generating Sets of Rotational Reidemeister Moves,* arXiv:2506.15628. See pp. 17.
[BZ] G. Burde and H. Zieschang, *Knots,* Walter de Gruyter, 2003. See pp. 31.
[Co] A. Conway, *The Levine-Tristram Signature: A Survey,* in 2019–20 MATRIX Annals, Springer 2021, arXiv:1903.04477. See pp. 23.
[CF] R. H. Crowell and R. H. Fox, *Introduction to Knot Theory,* Springer-Verlag GTM **57** (1963). See pp. 27.
[CDGW] M. Culler, N. Dunfield, M. Goerner, and J. Weeks, *SnapPy, a computer program for studying the geometry and topology of 3-manifolds,* http://snappy.computop.org. See pp. 24.
[Dr] V. G. Drinfel'd, *Quantum Groups,* Proc. Int. Cong. Math., 798–820, Berkeley, 1986. See pp. 29.
[DHOEBL] N. Dunfield, A. Hirani, M. Obeidin, A. Ehrenberg, S. Bhattacharyya, D. Lei, and others, *Random Knots: A Preliminary Report,* lecture notes at https://nmd.web.illinois.edu/slides/random_knots.pdf. Also a data file at https://drorbn.net/AcademicPensieve/People/Dunfield/nmd_random_knots. See pp. 5.
[FM] R. H. Fox and J. W. Milnor, *Singularities of 2-Spheres in 4-Space and Cobordism of Knots,* Osaka J. Math. **3-2** (1966) 257–267. See pp. 31.
[Gar] S. Garoufalidis, *Whitehead Doubling Persists,* Alg. & Geom. Top. **4** (2004) 935—942, arXiv:math/0003189. See pp. 28, 35.
[GK] S. Garoufalidis and R. Kashaev, *Multivariable Knot Polynomials from Braided Hopf Algebras with Automorphisms,* arXiv:2311.11528. See pp. 25.
[GL] S. Garoufalidis and S. Y. Li, *Patterns of the V_2-Polynomial of Knots,* arXiv:2409.03557. See pp. 25.
[GR] S. Garoufalidis and L. Rozansky, *The Loop Expansion of the Kontsevich Integral, the Null-Move, and S-Equivalence,* arXiv:math.GT/0003187. See pp. 1, 28.
[Gas] B. J. Gassner, *On Braid Groups,* Ph.D. thesis, New York University, 1959. See pp. 32.
[GST] R. E. Gompf, M. Scharlemann, and A. Thompson, *Fibered Knots and Potential Counterexamples to the Property 2R and Slice-Ribbon Conjectures,* Geom. and Top. **14** (2010) 2305–2347, arXiv:1103.1601. See pp. 25, 26.
[Ju] A. Juhász, *A Survey of Heegaard Floer Homology,* in New Ideas in Low Dimensional Topology, Series on Knots and Everything **56** (2015) 237–296. See pp. 32.
[Kau1] L. H. Kauffman, *On knots,* Princeton Univ. Press, Princeton, 1987. See pp. 31.
[Kau2] L. H. Kauffman, *Virtual Knot Theory,* European J. Comb. **20** (1999) 663–690, arXiv:math.GT/9811028. See pp. 28.
[Kau3] L. H. Kauffman, *Rotational Virtual Knots and Quantum Link Invariants,* J. of Knot Theory and its Ramifications **24-13** (2015), arXiv:1509.00578. See pp. 27, 28.
[Kaw] A. Kawauchi, *A Survey of Knot Theory,* Birkhauser Verlag, 1996. See pp. 32.
[Kh] M. Khovanov, *A Categorification of the Jones Polynomial,* Duke Mathematical Journal **101-3** (2000) 359–426, arXiv:math.QA/9908171. See pp. 32.
[Kr] A. Kricker, *The Lines of the Kontsevich Integral and Rozansky's Rationality Conjecture,* arXiv:math/0005284. See pp. 1, 28.
[Lal] A. K. Lalani, *A Computational Survey of the Theta Invariant,* GitHub repository, https://github.com/AliKarimLalani/theta_invariant. See pp. 2.
[Law] R. J. Lawrence, *Universal Link Invariants using Quantum Groups,* Proc. XVII Int. Conf. on Diff. Geom. Methods in Theor. Phys., Chester, England, August 1988. World Scientific (1989) 55–63. See pp. 29.
[Le] J. Levine, *Knot cobordism groups in codimension two,* Comment. Math. Helv. **44** (1969) 229—244. See pp. 23.
[Li] W. B. R. Lickorish, *An Introduction to Knot Theory,* Springer-Verlag GTM **175** (1997). See pp. 27.
[LM] C. Livingston and A. H. Moore, *KnotInfo: Table of Knot Invariants,* http://knotinfo.org, August 26, 2025. See pp. 25, 26.
[LV] D. López Neumann and R. van der Veen, *Non-Semisimple sl_2 Quantum Invariants of Fibred Links,* Adv. in Math. **480A** (2025), arXiv:2407.15561. See pp. 26.
[Ma] C. Manolescu, *An Introduction to Knot Floer Homology,* in Physics and Mathematics of Link Homology, Contemporary Mathematics, Centre de Recherches Mathématiques Proceedings **680** (2016) 89–135. See pp. 32.
[Oh1] T. Ohtsuki, *Quantum Invariants,* Series on Knots and Everything **29**, World Scientific 2002. See pp. 29.
[Oh2] T. Ohtsuki, *On the 2-Loop Polynomial of Knots,* Geometry & Topology **11** (2007) 1357–1475. See pp. 1, 28, 31.
[Oh3] T. Ohtsuki, *A Cabling Formula for the 2-Loop Polynomial of Knots,* Publ. RIMS, Kyoto University **40** (2004) 949–971, arXiv:math/0310216. See pp. 28, 29.
[OS] P. Ozsváth and Z. Szabó, *An Introduction to Heegaard Floer Homology,* Clay Mathematics Proceedings **5** (2004) 3–27. See pp. 32.
[Ov] A. Overbay, *Perturbative Expansion of the Colored Jones Polynomial,* Ph.D. thesis, University of North Carolina, August 2013, https://cdr.lib.unc.edu/concern/dissertations/hm50ts889. See pp. 24, 28.
[Po1] M. Polyak, *Feynman Diagrams for Pedestrians and Mathematicians,* arXiv:math/0406251. See pp. 30.
[Po2] M. Polyak, *Minimal Generating Sets of Reidemeister Moves,* Quantum Topol. **1** (2010) 399–411, arXiv:0908.3127. See pp. 15.
[Rol] D. Rolfsen, *Knots and Links,* AMS Chelsea, 2003. See pp. 26.
[Roz1] L. Rozansky, *A Contribution of the Trivial Flat Connection to the Jones Polynomial and Witten's Invariant of 3D Manifolds, I,* Comm. Math. Phys. **175-2** (1996) 275–296, arXiv:hep-th/9401061. See pp. 1, 24, 28.
[Roz2] L. Rozansky, *The Universal R-Matrix, Burau Representation and the Melvin-Morton Expansion of the Colored Jones Polynomial,* Adv. Math. **134-1** (1998) 1–31, arXiv:q-alg/9604005. See pp. 1, 24, 28.
[Roz3] L. Rozansky, *A Universal U(1)-RCC Invariant of Links and Rationality Conjecture,* arXiv:math/0201139. See pp. 1, 24, 28.
[Sch] S. Schaveling, *Expansions of Quantum Group Invariants,* Ph.D. thesis, Universiteit Leiden, September 2020, https://scholarlypublications.universiteitleiden.nl/handle/1887/136272. See pp. 29.
[Tr] A. Tristram, *Some cobordism invariants for links,* Proc. Cambridge Philos. Soc. **66** (1969) 251—264. See pp. 23.
[Wo] *Wolfram Language & System Documentation Center,* https://reference.wolfram.com/language/. See pp. 8.

Added after submission, remove once settled:

- On 250930. Added [Gar] and the sentence at the end of Discussion 26.

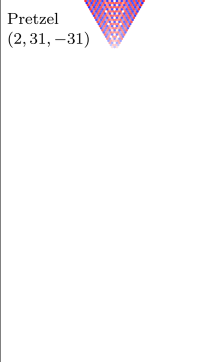

Pretzel
$(2, 31, -31)$

Department of Mathematics, University of Toronto, Toronto Ontario M5S 2E4, Canada
Email address: drorbn@math.toronto.edu
URL: http://www.math.toronto.edu/drorbn

University of Groningen, Bernoulli Institute, P.O. Box 407, 9700 AK Groningen, The Netherlands
Email address: roland.mathematics@gmail.com
URL: http://www.rolandvdv.nl/